Int. J. Heat Mass Transfer. Vol. 28, No. 3, pp. 523–529, 1985
Printed in Great Britain

0017-9310/85 $3.00 + 0.00

Conjugate mixed convection and conduction heat transfer along a vertical circular pin

MING-JER HUANG and CHA'O-KUANG CHEN
Department of Mechanical Engineering, National Cheng Kung University, Tainan, Taiwan, Republic of China

(*Received* 26 *March* 1984 *and in revised form* 27 *July* 1984)

Abstract—The heat transfer characteristics of laminar mixed convection flow over a vertical pin are studied analytically by conjugate convection–conduction theory. Numerical results for the local heat transfer coefficient, local heat flux, efficiency, and temperature distributions of pin under the effects of surface curvature, the buoyancy force parameter and the conjugate convection–conduction parameter, are obtained by solving simultaneously the convective boundary layer equations of the fluid and energy equations of the pin. The results of the present numerical solution have been compared with those of the conventional fin theory. It is found that there is some discrepancy between the pin efficiency and the temperature distribution.

INTRODUCTION

RECENTLY, the conjugate convection and conduction problems for a vertical plate fin have been analyzed by Sparrow and Acharya [1], Sparrow and Chyu [2], and Sunden [3]. They concluded that the conventional fin model based on a uniform value of the heat transfer coefficient yields very good predictions for the rate of overall heat transfer of the fin, but cannot predict the local heat fluxes. Even in the natural convection flow, the local heat transfer coefficients were found not to decrease monotonically in the flow direction, as is usual. Rather, the coefficient decreased at first, attained a minimum, and then increased with increasing downstream distance. Therefore, determination of the true heat transfer coefficient along the surface is necessary.

In the present investigation, attention is focused on the analysis of mixed convection flow over a vertical circular pin fin, which is extended from a wall. Since the temperature of the pin is not known *a priori* (it is affected by the heat transfer coefficient) the coefficient is also dependent on the ambient fluid flow. Hence, it is necessary to solve the conjugate convection and conduction problem. The problem can be separated into two parts. One is the conservation equations of the laminar mixed convection boundary layer flow field, and the other is the energy equation of the pin itself. The mixed convection flow over a vertical circular pin does not admit simiiarity solutions. The nonsimilarities arise from the transverse curvature of the cylinder, the buoyancy force and the nonuniform temperature distributions which are to be determined. In addition, owing to the presence of the buoyancy force, the flow and thermal field are coupled. An implicit finite difference method is employed to solve the transformed nonsimilar equations.

The pin considered is long compared with its diameter, and the pin temperature variations in the longitudinal direction can be considered to be much larger than those in the transverse direction. Hence, it may be assumed that heat conduction along the pin is essentially one-dimensional. In addition, the amount of heat which is convected from the tip of the pin to the fluid is smaller than those of the other parts of the pin. Therefore, the tip of the pin can be reasonably considered as adiabatic.

The assumed pin temperature distributions, which are based on the conventional pin theory, serve as boundary conditions for the boundary layer equations. The solutions of the local heat transfer coefficient along the pin surface from the boundary layer equations are resubstituted into the pin energy equation in search of the new temperatures of pin surface. Thus, these new temperature distributions are then imposed as the surface boundary conditions for the boundary layer equations, the solutions of which are used to evaluate an updated h, and so on until the maximum difference of temperature between the successive iterations is less than a given small value of (10^{-4}).

Numerical results of interest, such as the local heat transfer coefficient, local heat flux, efficiency, and distributions of temperature along the pin surface are presented for air with a Prandtl number of 0.7, buoyancy force parameters, $Gr/Re^2 = 0.0$, 3.0, and 5.0, conjugate convection–conduction parameters, $Nc = 0.5$ and 5.0, and transverse curvature parameters, $\lambda = 1.0$ and 3.0.

ANALYSIS

Consider a vertical circular pin of radius r_0 and length L which is attached to a wall of temperature T_0 and is aligned parallel to a uniform free stream with velocity U and temperature T_∞. The axial and radial coordinates are taken to be x and r, with x measuring the distance along the centerline of the cylinder. Let the

NOMENCLATURE

f	dimensionless stream function
Gr	Grashof number, $g\beta(T_0-T_\infty)L^3/v^2$
g	gravitational acceleration
h	heat transfer coefficient
$\hat{h}$	dimensionless heat transfer coefficient, $hL/k_f Re^{1/2}$
k	thermal conductivity
L	pin length
Nc	conjugate convection–conduction parameter, $2Lk_f Re^{1/2}/k_s r_0$
Pr	Prandtl number, v/α
q	local heat flux
Re	Reynolds number, UL/v
r	radial coordinate
r_0	radius of pin
T	temperature
T_0	pin base temperature
U	free stream velocity
u, v	velocity components in the x and r coordinates, respectively
x	streamwise coordinate.

Greek symbols

α	thermal diffusivity
β	coefficient of volumetric expansion
η	pseudo-similarity variable, $(r^2-r_0^2)(Re/\xi)^{1/2}/4r_0L$
η_f	thermal efficiency of pin
θ	dimensionless temperature
λ	transverse curvature parameter, $4L/r_0 Re^{1/2}$
v	kinematic viscosity
ξ	dimensionless pin length, x/L
ψ	stream function.

Subscripts

s	condition at the pin surface
w	condition at the wall
∞	condition at infinity.

gravitational force act in the opposite direction to the x coordinate. The buoyancy force then acts in the same direction as the forced flow when $T_0 > T_\infty$. The thermal conductivity of the pin is k_s and that of the fluid is k_f. The physical properties are assumed to be constant except the fluid density, which is employed by the Boussinesq approximation. The conservation equations of the laminar boundary layer can be expressed as [4]:

$$\frac{\partial}{\partial x}(ru)+\frac{\partial}{\partial r}(rv)=0 \tag{1}$$

$$u\frac{\partial u}{\partial x}+v\frac{\partial u}{\partial r}=g\beta(T-T_\infty)+\frac{v}{r}\frac{\partial}{\partial r}\left(r\frac{\partial u}{\partial r}\right) \tag{2}$$

$$u\frac{\partial T}{\partial x}+v\frac{\partial T}{\partial r}=\frac{\alpha}{r}\frac{\partial}{\partial r}\left(r\frac{\partial T}{\partial r}\right) \tag{3}$$

where the notations are defined in the nomenclature.

The system of equations (1)–(3) is subject to the following boundary conditions

$$\left.\begin{array}{l} u=v=0,\quad T=T_w(x)\quad \text{at}\quad r=r_0 \\ u\to U,\quad T\to T_\infty\quad \text{at}\quad r\to\infty \\ u=U,\quad T=T_\infty\quad \text{at}\quad x=0,\quad r\geqslant r_0. \end{array}\right\} \tag{4}$$

Equations (1)–(3) and boundary conditions (4) do not admit similarity solutions. The nonsimilarities arise from the surface curvature of the pin, the buoyancy force effect and the nonuniform temperature distribution of the pin. As the first step in the analysis, these equations and boundary conditions are transformed into a dimensionless form. One introduces the pseudo-similarity variable η and the dimensionless axial coordinate ξ as follows.

$$\xi=x/L,\quad \eta=\frac{r^2-r_0^2}{4r_0L}(Re/\xi)^{1/2} \tag{5}$$

along with the dimensionless stream function $f(\xi,\eta)$ and the dimensionless temperature $\theta(\xi,\eta)$ defined, respectively, by

$$f(\xi,\eta)=\psi(x,r)/[r_0(vUx)^{1/2}] \tag{6}$$

$$\theta(\xi,\eta)=[T(x,r)-T_\infty]/(T_0-T_\infty) \tag{7}$$

where the stream function $\psi(x,r)$ automatically satisfies the continuity equation (1) with

$$ru=\frac{\partial\psi}{\partial r},\quad rv=-\frac{\partial\psi}{\partial x}. \tag{8}$$

Substituting equations (5)–(7) into equations (2)–(4), one obtains

$$(1+\xi^{1/2}\lambda\eta)f'''+(f+\xi^{1/2}\lambda)f''+8\xi\, Gr\, Re^{-2}\,\theta = 2\xi\left(f'\frac{\partial f'}{\partial\xi}-f''\frac{\partial f}{\partial\xi}\right) \tag{9}$$

$$Pr^{-1}(1+\xi^{1/2}\lambda\eta)\theta''+(f+Pr^{-1}\xi^{1/2}\lambda)\theta' = 2\xi\left(f'\frac{\partial\theta}{\partial\xi}-\theta'\frac{\partial f}{\partial\xi}\right) \tag{10}$$

$$\begin{array}{c} f(\xi,0)=f'(\xi,0)=0,\quad \theta(\xi,0)=\theta_w(\xi) \\ f'(\xi,\infty)=2,\quad \theta(\xi,\infty)=0. \end{array} \tag{11}$$

In the foregoing equations, the primes stand for partial derivatives with respect to η, Pr is the Prandtl number, Gr is the Grashof number, Re is the Reynolds number, and λ is the transverse curvature parameter, defined as

$$\lambda = 4L/r_0\, Re^{1/2}. \quad (12)$$

Assuming a one-dimensional model the thin pin energy equation can be written as, in dimensionless form

$$\frac{d^2\theta_s}{d\xi^2} = Nc\hat{h}\theta_s \quad (13)$$

where θ_s is the dimensionless pin temperature, $\hat{h}$ is the dimensionless form of local heat transfer coefficient, and Nc is the conjugate convection–conduction parameter. They are defined, respectively, as follows

$$\theta_s(\xi) = [T_s(x) - T_\infty]/(T_0 - T_\infty) \quad (14)$$

$$\hat{h}(\xi) = [-\theta'/\theta]_{\eta=0}/2\xi^{1/2} \quad (15)$$

$$Nc = 2Lk_f\, Re^{1/2}/k_s r_0. \quad (16)$$

Equation (13) has to be solved with respect to boundary conditions.

$$\begin{aligned} d\theta_s/d\xi &= 0 \quad \text{at} \quad \xi = 0 \\ \theta_s &= 1 \quad \text{at} \quad \xi = 1. \end{aligned} \quad (17)$$

Of particular interest is the thermal coupling between the pin and the convective boundary layer. The basic coupling is expressed by the requirement that the pin, fluid temperatures and heat fluxes be continuous at the pin–fluid interface, at all x.

$$T_s(x) = T_w(x)$$

$$h(T_s - T_\infty) = -k_f \left.\frac{\partial T}{\partial r}\right|_{r=r_0}$$

$$\text{at} \quad r = r_0, \quad 0 \leqslant x \leqslant L. \quad (18)$$

NUMERICAL SOLUTION

The solution begins by solving the convective boundary layer problem for a vertical circular pin with guessed temperature for all ξ. In order to reduce the number of iterations, we use the guessed temperature distributions, $\theta_s(\xi) = \cosh(Nc\xi)/\cosh(Nc)$ which is based on the conventional theory, to start the numerical solution. The dimensionless heat transfer coefficients determined from this solution in accordance with equation (15) are then used as input to the pin heat conduction equation (13). With Nc prescribed, the differential equation (13) is then solved to yield $\theta_s(\xi)$.

To begin the next cycle of the iterative procedure, the just-determined $\theta_s(\xi)$ is imposed as the thermal boundary condition for the convective boundary layer problem; the solution to which yields a new $\hat{h}(\xi)$ distribution which is used as input to the pin heat conduction equation. This procedure of alternately solving the boundary layer problem and the pin conduction problem is continued until convergence is attained.

The two systems of partial differential equations (9), (10) are coupled. In the present study, these equations were solved by an accurate implicit finite difference technique. This technique is a modified version of the method described in [5] for the solution of uncoupled equations. To begin with, the partial differential equations (9), (10) are first converted into a system of first-order equations which are then expressed in finite difference form by approximating the functions and their first derivatives in terms of centred difference and averages at midpoints of the net segments in the (ξ, η) coordinates. The resulting nonlinear finite difference equations are then solved by Newton's iterative method.

The boundary layer solutions were obtained by a marching procedure, starting at the leading edge ($\xi = 0$) and the grids were divided into 45 points in the stream direction. There was a denser concentration of points near the leading edge to accommodate the initial rapid growth of the boundary layer. Owing to the transverse curvature effect, a variable grid (rather than a uniform grid) normal to the flow is used.

The pin conduction equation was solved by using the direct inverse matrix method. The pin equation was also divided into 45 grid points and expressed in finite difference form. To ensure high accuracy, nonuniform grid points were used. For smaller ξ, a finer ξ subdivision was needed for the boundary layer solution.

To confirm the accuracy of the present numerical method, its results have been compared and found to be in good agreement with those of the nonsimilarity solution [4] for the mixed convection flow over a vertical isothermal cylinder.

In order to reveal the heat transfer characteristics of the real pin, the characteristics of the conventional fin theory, which is based on a uniform heat transfer coefficient, are also calculated. If $\hat{h}$ is regarded as a known mean value, which is given by the available boundary layer equations (9)–(11) subjected to isothermal pin surface temperature, then equation (13) does not couple with the fluid flow and can be analytically solved.

RESULTS AND DISCUSSION

Representative distributions of the dimensionless local heat transfer coefficients along the pin surface under the effects of surface transverse curvature, $\lambda = 1.0$ and 3.0, buoyancy force, $Gr/Re^2 = 0.0$, 3.0, and 5.0, and conjugate convection–conduction parameter, $Nc = 0.5$ and 5.0, are shown in Figs. 1 and 2, respectively. They reveal that for a given λ and $Gr/Re^2 = 0.0$ (pure forced convection) the coefficients always tend to decrease monotonically from the infinite value at the tip to the same value at the root for all Nc. The larger Nc, representing the greater temperature variations of the pin, has the higher local heat transfer coefficient. However, as the buoyancy force increases the coefficient no longer decreases along the direction of the fluid flow, but decreases at first to a minimum value, and then increases. It will be obvious that as the

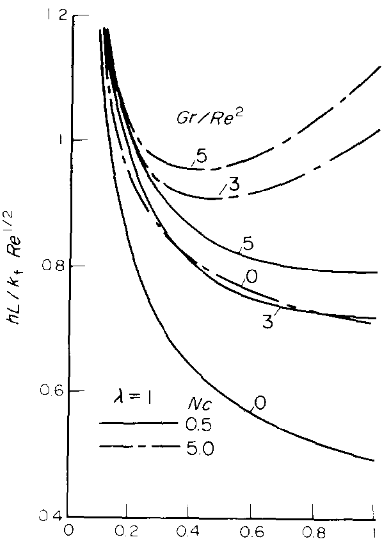

FIG. 1. Local heat transfer coefficients.

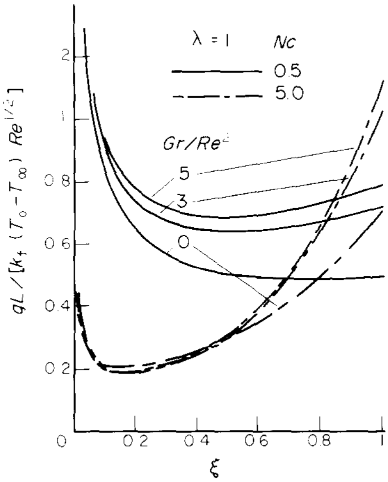

FIG. 3. Local heat fluxes.

conjugate convection–conduction parameter increases, the location of the minimum shifts toward the tip and the extent of the downstream rise becomes greater. These behaviours obtained in the present work are similar to those of the flat plate fin reported by [1–3].

Distributions of the dimensionless local heat fluxes along the pin surface are illustrated in Figs. 3 and 4, respectively, for $\lambda = 1.0$ and 3.0. Each figure contains $Gr/Re^2 = 0.0$, 3.0, and 5.0 and $Nc = 0.5$ and 5.0. The dimensionless local heat fluxes can be taken as

$$qL/[K_f(T_0 - T_\infty)\,Re^{1/2}] = -\theta'(\xi, 0)2\xi^{1/2}. \quad (19)$$

From the figures, under a given transverse curvature parameter λ, the buoyancy force increases the local heat fluxes for all major parts of the pin surface. However, in the vicinity of the tip the influence of the buoyancy force is very small. As Nc increases, most of the heat flux passes to the fluid in the neighbourhood of root. It can explain that the larger Nc, representing the lower thermal conductivity of pin, the higher temperature exists near the root. In all Nc, the infinite heat flux still exists at $\xi = 0$, since it is a singular point.

If the results in Fig. 3 are compared with those in Fig. 4, it can be seen that the local heat fluxes for the large surface curvature are higher than those of the small surface curvature. However, one should note that the radius of the pin is not the same for $\lambda = 1$ and $\lambda = 3$. Thus, the smaller values of local heat fluxes for $\lambda = 1$ do not mean that the total heat fluxes over the pin surface are less than those of $\lambda = 3$, which is of larger radius of pin.

The area under the curve of the local heat flux represents the total heat transfer rate convected from the pin surface to the fluid. It can also be obtained from

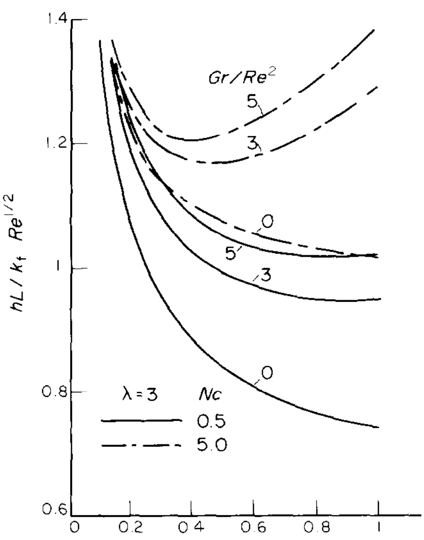

FIG. 2. Local heat transfer coefficients.

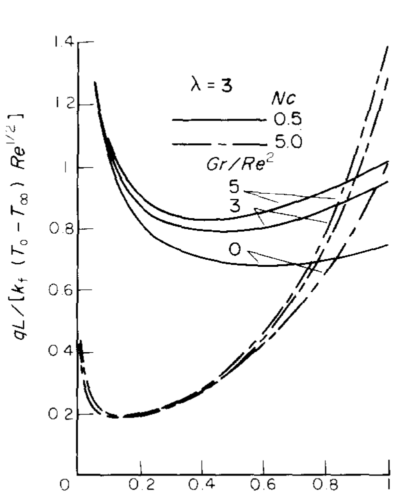

FIG. 4. Local heat fluxes.

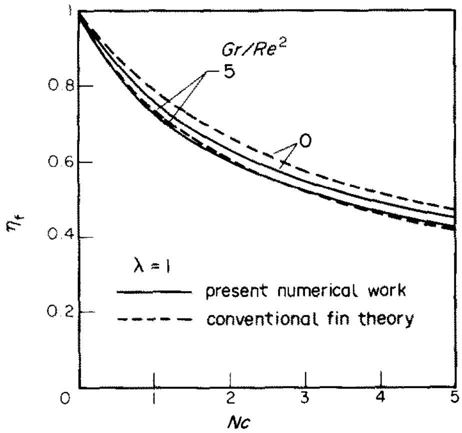

FIG. 5. The efficiency of the pin.

the heat conducted from the wall into the pin base ($\xi = 1$). The corresponding total heat transfer rate of these two methods should be in agreement.

A major interest of the present investigation is in the analysis of the thermal boundary layer effects on an actual pin. Hence, the analysis of the pin is different from that of conventional fin theory which only considers a uniform heat transfer coefficient along the pin surface. The efficiency of the pin is defined as the ratio of the actual heat transfer rate of the pin to that of an isothermal pin. The efficiencies of these two models are plotted in Figs. 5 and 6 as a function of conjugate convection–conduction parameter Nc. For each figure, the dashed lines represent the results of the conventional fin theory and the solid lines correspond to the present numerical solution. As confirmation, the curves are all downwards with increasing values of Nc, which shows the smaller pin conductivity promotes the greater pin temperature variations and lower values of the efficiency. From the figures, it can be seen that the efficiency of the conventional fin theory is higher than that of the present numerical solution. It is also shown that between these two models the difference is higher in pure convection ($Gr/Re^2 = 0.0$) than in mixed convection flow. Thus, from an engineering point of view, the simple conventional fin theory is of more use in mixed convection than in pure forced convection.

Since the buoyancy force assists the forced flow, the convective heat transfer is increased, resulting in lower pin temperatures and smaller pin efficiencies. If the results in Fig. 5 are compared with those in Fig. 6, the effects of the surface curvature on the efficiency can be seen. The smaller the surface curvature, the larger the radius of the pin which has higher efficiency and a smaller nonuniformity of temperature.

The results for the pin temperature distribution are presented in Figs. 7 and 8 for the two transverse surface curvatures, $\lambda = 1$ and 3, respectively. Each figure also includes the results of the conventional fin theory model and the present numerical work. The pin temperature distributions are functions of Nc and Gr/Re^2. They all show the expected trend whereby the pin temperature distributions decrease monotonically from the root to the tip. But the temperatures calculated by the conventional fin theory are always higher than those of the present numerical solution. It also confirms the previous statements that the larger values of Nc, Gr/Re^2 and λ give rise to the greater pin temperature variations.

The surface curvature effect on the local heat transfer coefficient is presented in Fig. 9. The dotted line represents the local heat transfer coefficient of the vertical flat plate fin (i.e. $\lambda = 0$). As inspection of Fig. 9 reveals that for given $Nc = 5.0$ and $Gr/Re^2 = 2.0$, the

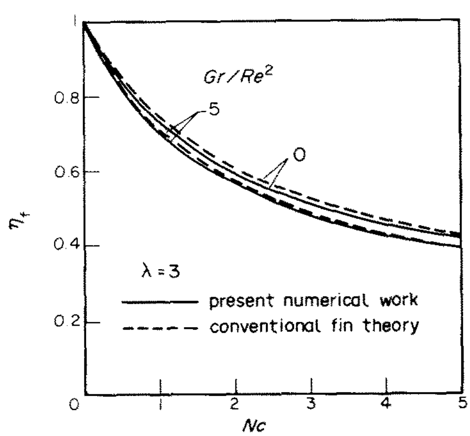

FIG. 6. The efficiency of the pin.

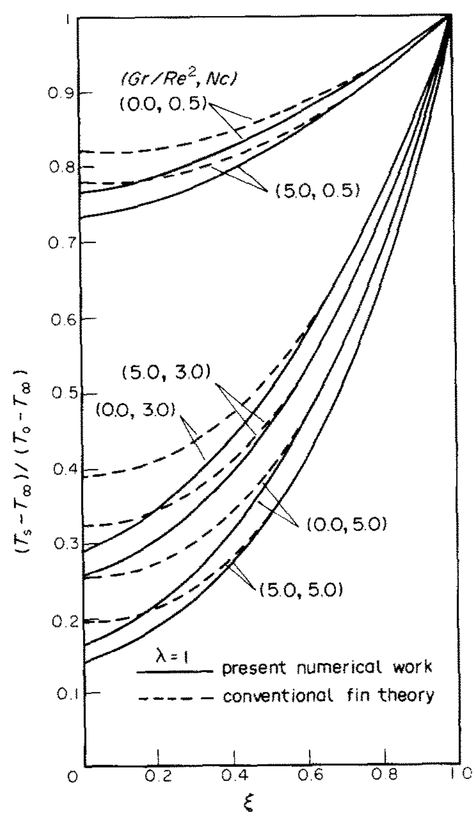

FIG. 7. Temperature distributions of the pin.

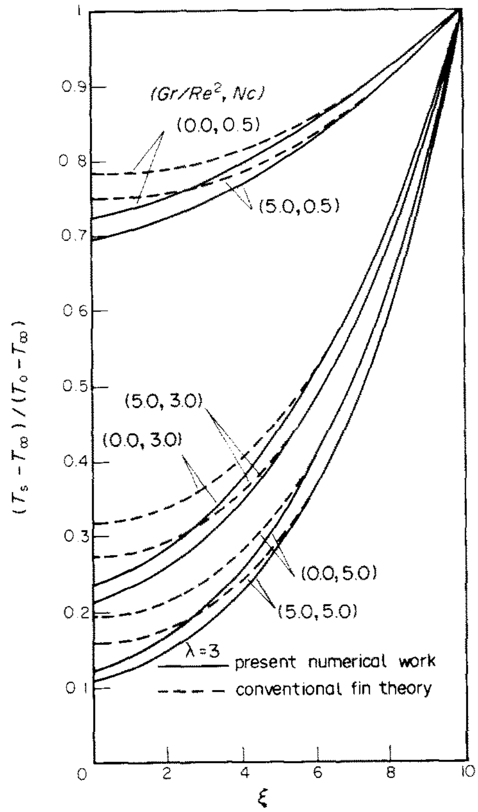

FIG. 8. Temperature distributions of the pin.

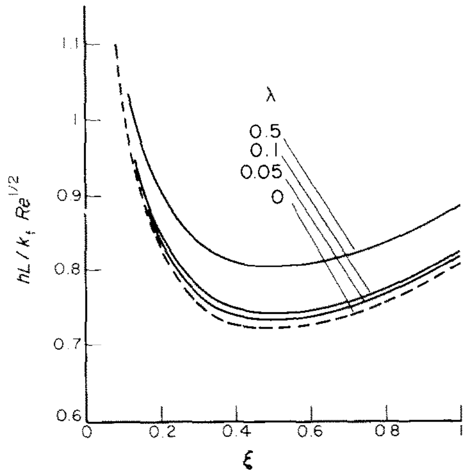

FIG. 9. Surface curvature effects on the heat transfer coefficient.

coefficient increases with increasing surface curvature λ. The maximum difference of the local heat transfer coefficient between the cylinder and the vertical plate fin is found to be less than 2% when $\lambda \leqslant 0.1$. For the case of a vertical flat plate fin, the present numerical solution can be reduced to $\lambda \leqslant 0.1$.

CONCLUSIONS

A study has been conducted to analyze the conjugate convection and conduction heat transfer characteristics of buoyancy force on the forced flow over a vertical circular pin. The analysis is restricted to the energy equation of the pin as a one-dimensional model. In general, it has been found that the smaller the thermal conductivity k_s, then the higher the heat transfer coefficients and the greater the surface temperature variations from the root to the tip. The overall heat transfer increases with increasing buoyancy force and decreases with increasing convection–conduction parameter.

REFERENCES

1. E. M. Sparrow and S. Acharya, A natural convection fin with a solution-determined nonmonotonically varying heat transfer coefficient, *J. Heat Transfer* **103**, 218–225 (1981).
2. E. M. Sparrow and M. K. Chyu, Conjugated forced convection–conduction analysis of heat transfer in a plate fin, *J. Heat Transfer* **104**, 204–206 (1982).
3. B. Sunden, Conjugate mixed convection heat transfer from a vertical rectangular fin, *Int. Comm. Heat Mass Transfer* **10**, 267–276 (1983).
4. T. S. Chen and A. Mucoglu, Buoyancy effects on forced convection along a vertical cylinder, *J. Heat Transfer* **97**, 198–203 (1975).
5. T. Cebeci and P. Bradshow, *Momentum Transfer in Boundary Layers*, Hemisphere Publishing, Washington D.C. (1977).

TRANSFERT THERMIQUE MIXTE PAR CONDUCTION ET CONVECTION LE LONG D'UNE AIGUILLE CIRCULAIRE VERTICALE

Résumé—Les caractéristiques de la convection thermique laminaire sur une aiguille verticale sont étudiées analytiquement par la théorie de convection et conduction couplées. Des résultats numériques pour le coefficient de transfert thermique local, le flux de chaleur local, l'efficacité et les distributions de température de l'aiguille sous l'effet de la courbure de la surface, le paramètre de gravité et le paramètre de couplage conduction–convection, sont obtenus en résolvant simultanément les équations de couche limite dans le fluide et de l'équation d'énergie dans l'aiguille. Les résultats de la solution numérique est comparée avec ceux de la théorie conventionnelle. On trouve qu'il y a un écart pour l'efficacité et la distribution de température.

WÄRMEÜBERTRAGUNG DURCH GEKOPPELTE MISCHKONVEKTION UND WÄRMELEITUNG LÄNGS EINER SENKRECHTEN, KREISRUNDEN STABRIPPE

Zusammenfassung—Die Wärmeübertragungs-Charakteristiken von laminarer Mischkonvektionsströmung an einer senkrechten Stabrippe werden rechnerisch anhand einer gekoppelten Konvektions-Wärmeleitungstheorie untersucht. Rechenergebnisse für den örtlichen Wärmeübergangskoeffizienten, die örtliche Wärmestromdichte, den Wirkungsgrad und die Temperaturverteilung in der Stabrippe unter dem Einfluß von Oberflächenkrümmung, Auftriebskraftparametern und gekoppelten Konvektions-Wärmeleitparametern werden durch simultane Lösung der Grenzschichtgleichungen der konvektiven Strömung des Fluids und der Energiegleichungen der Stabrippe ermittelt. Die Ergebnisse der beschriebenen numerischen Lösung werden mit solchen aus der konventionellen Rippentheorie verglichen. Es zeigt sich, daß es einige Unterschiede beim Rippenwirkungsgrad und bei der Temperaturverteilung gibt.

СОПРЯЖЕННЫЙ ТЕПЛОПЕРЕНОС СМЕШАННОЙ КОНВЕКЦИЕЙ И ТЕПЛОПРОВОДНОСТЬЮ ВДОЛЬ ВЕРТИКАЛЬНОГО КРУГЛОГО СТЕРЖНЯ

Аннотация—С помощью сопряженной теории смешанной конвекции изучены характеристики теплопереноса ламинарного течения вдоль вертикального стержня. Путем одновременного решения уравнений конвективного пограничного слоя для жидкости и уравнения энергии для стержня получены численные значения коэффициента локального теплопереноса, локального теплового потока, интенсивности теплообмена и распределения температуры стержня в зависимости от кривизны поверхности, коэффициента подъемной силы и параметра, описывающего сопряженный теплообмен. Полученные результаты численного расчета сравниваются с общепринятой теорией ребра. Найдено, что имеет место некоторое расхождение для интенсивности теплообмена стержня и распределения температуры.